Level structure of the double-shell closure system with $Z = 14$ and $N = 20$: ^{34}Si*

Chang-Bum Moon[1†]   Cenxi Yuan(袁岑溪)[2‡]

[1]Center for Exotic Nuclear Studies, The Institute for Basic Science (IBS), Daejeon 34126, Republic of Korea
[2]Sino-French Institute of Nuclear Engineering and Technology, Sun Yat-Sen University, Zhuhai 519082, China

Abstract: The level structure of the double-magic nucleus ^{34}Si ($Z = 14$, $N = 20$) was investigated by evaluating the available data. On the basis of experimental results from the beta-decay and fusion-evaporation reactions, we established the level scheme by assigning spin-parities up to 6_1^+ at 6233 keV. The high energy positions of the excited states are consistent with the magicity at ^{34}Si, such as the 2_2^+ state of the spherical ground band at 4.519 MeV and the 3^-, 4^-, and 5^- states of the one-particle one-hole cross-shell states at approximately 4.5 MeV. This nucleus, for a long time, has attracted much attention because of, on one side, a proton bubble structure in the ground state and, on the other side, a deformation in the second 0^+ state, 0_2^+. By a comparison of the constructed level scheme with the shell model calculations, we describe the emerging structures in the ground and second 0^+ states and the negative-parity 3^- states within the framework of the shell model context. We propose a deformed rotational band with the cascading $6_2^+ - 4_1^+ - 2_1^+$ transitions built on the 0_2^+ state.

Keywords: double shell closure, level scheme, two particle-two hole excitations, large-scale shell model calculations

DOI: 10.1088/1674-1137/ac8a8c

I. INTRODUCTION

Historically, magic nuclei are famous, similar to inert gas elements. The emergence of a large shell gap leads to more stability for these nuclei in comparison with neighboring nuclei. By introducing a strong spin-orbital coupling term into the single-particle potential, the magic numbers could finally be reproduced, such as 28, 50, 82, and 126. The corresponding spin (s)-orbital (l) doublets involved in generating these numbers are $f_{7/2}$-$f_{5/2}$ ($l = 3$), $g_{9/2}$-$g_{7/2}$ ($l = 4$), $h_{11/2}$-$h_{9/2}$ ($l = 5$), and $i_{13/2}$-$i_{11/2}$ ($l = 6$), respectively. Here, l denotes the angular momentum number, and the subscript indicates the total spin number, $j = l \pm s$. Notice that those are the highest l value orbitals for each harmonic oscillator (principal) number N. In addition, the numbers of 14 and 6, which are based on shell gaps due to splits of the $d_{5/2}$-$d_{3/2}$ ($l = 2$) and $p_{3/2}$-$p_{1/2}$ ($l = 1$) orbitals, should be regarded as magic numbers as well.

The nuclei ^{14}C ($Z = 6$, $N = 8$), ^{34}Si ($Z = 14$, $N = 20$), and ^{68}Ni ($Z = 28$, $N = 40$) have a common shell character; proton magic-numbers occur due to spin-orbital splits, while neutron numbers occur due to harmonic oscillator shell gaps. From these, we examine the level structure of ^{34}Si. To date, the excited states of ^{34}Si have been identified for an energy of up to $E_x = 6233$ keV, but the spin-parity assignment has been made only for the first 2^+, 3^- and the second 0^+, 2^+ states [1−7]. Moreover, no overall study of the level structure of this nucleus has been made. Instead, most studies are concerned with identifying the second 0^+ state to prove the deformed $2\hbar\omega$ pf-shell nature [2−11] and the bubble matter distribution of the protons in the spherical ground state [12−14]. In this work, we first construct the level scheme from existing data, then compare it to those of the neighboring isotones with $N = 20$ and finally discuss the underlying shell and collective structures using large-scale shell-model approaches.

II. AVAILABLE DATA ANALYSIS

Figure 1 shows the currently-known level scheme of ^{34}Si. The 2^+ and 3^- states were firstly identified through the β-decay of ^{34}Al [2−4]. The levels at 4379 and 4969 keV were tentatively assigned (3^-, 4^-, 5^-) on the basis of logft values [4]. The 4519 keV level was also observed in β-decay measurements [4, 8]. Conversely, the levels at 4920 and 6233 keV were observed only in a fusion-evap-
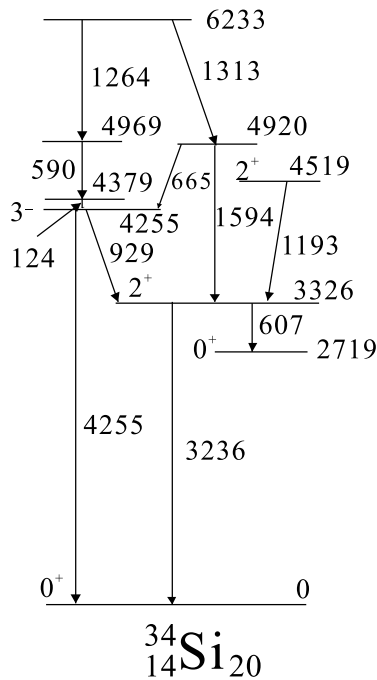
Fig. 1. A partial level scheme of ^{34}Si as observed from the β-decay of ^{34}Al [2−4, 6] and the results of in-beam gamma-ray spectroscopy of the ^{18}O(^{18}O, 2p)^{34}Si reaction [5].

oration reaction, ^{18}O (^{18}O, 2p) ^{34}Si [5]. The second 0^+ at 2719 keV, including the populated 607-keV transition, has been identified using positron-electron internal pair-creation spectroscopy on the β-decay of ^{34}Al [6].

By looking closely at the γ-ray transitional properties of the ^{18}O (^{18}O, 2p) ^{34}Si reaction [5], we are able to assign spin-parities with an argument concerning fusion-evaporation reactions. Generally, the fusion-evaporation reaction yields mainly yrast states, which are the lowest

levels in energy for a given spin. According to the γ-ray intensities from a given level scheme in Ref. [5], the yrast states were found to be along the 6233 - 4969 - 4379 - 4255 (3$^-$) - 3326 (2$^+$) keV line. Thus, the 4379, 4969, and 6233 keV levels could be assigned the spins J = 4, 5, and 6, respectively. Among them, the 4379 and 4969 keV levels were suggestive of negative parity states, possibly (3$^-$,4$^-$,5$^-$) from β-decay measurements [1, 4]. Accordingly, we propose the 4969 and 4379 keV levels to be 5$^-$ and 4$^-$, respectively. We find that the 1594-keV transition from the 4920 keV to the 2$^+$ level at 3326 keV is relatively strong in intensity. Further, the 4920-keV level has another branch with a weak intensity connected to the 3$^-$ state at 4255 keV. Consequently, the 4920-keV level is supposed to have spins of 4 rather than of 3. Considering the higher probability of E2 than M2 transitions, we assign the 4920- and 6233-keV levels to be 4$^+$ and 6$^+$, respectively. Finally, let us look at the 4519-keV level with a 1193-keV transition connected to the 2$^+$ state at 3326 keV. The 1193-keV transition has been observed in both β-decay and in-beam fusion-evaporation γ-ray measurements. Further, this transition was also seen in the β-decay of the 1$^+$ isomer of ^{34}Al from the precursor ^{34}Mg nucleus [8]. Thereby, a spin assignment of 3 should be excluded. Moreover, observation from the in-beam reaction [5] excludes the possibility of 0$^+$ or 1$^+$. Eventually, this level must be 2$^+$. Our assignment is certainly consistent with the recent result by Han *et al.* [9].

We show the constructed level scheme of ^{34}Si in Fig. 2, in which the level schemes of the isotones ^{36}S and ^{38}Ar are also included. At first glance, a similarity appears for the negative-parity states 3$^-$, 4$^-$, and 5$^-$.

As will be discussed below, these negative-parity states are associated with neutron one particle-one hole
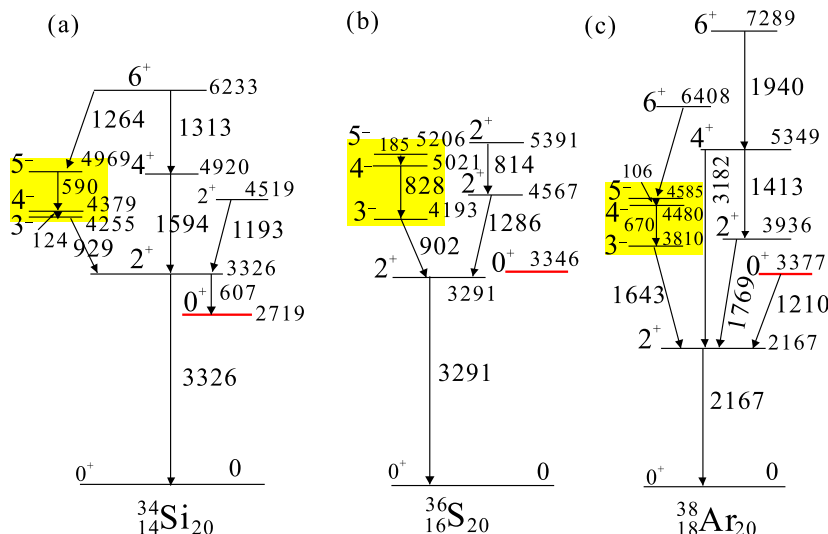

Fig. 2. (color online) The level schemes of ^{34}Si (a) as obtained from the present work, ^{36}S (b), and ^{38}Ar (c) [1]. For comparison, the negative states are denoted in yellow.

excitations across the $N = 20$ shell gap. What we notice next is that the second 2^+ states show a similar property, connecting the first 2^+ states. Despite no observation of the 4^+ state in ^{36}S, the 4^+ and 6^+ states of ^{34}Si show a similar pattern to those of ^{38}Ar. Overall, we conclude that our spin assignments of the observed excited states in ^{34}Si are reasonable. In addition, as we will see later, the large-scale shell-model calculations prove that the present result is correct.

III. CALCULATIONS AND DISCUSSION

To explain the underlying nuclear structure of the presented level scheme of ^{34}Si, we performed theoretical calculations with a large-scale shell model. The space spans over $d_{5/2}$, $s_{1/2}$, $d_{3/2}$, $f_{7/2}$, and $p_{3/2}$ for both protons and neutrons. The used effective shell-model interaction was sdpf-m [15]. The calculations were performed with the shell-model code, KSHELL [16, 17]. In this calculation, up to three particle-three hole $(0 - 3\ \hbar\omega)$ configurations were employed. It is found that the neutron cross-shell excitations are rather dominant over the protons, leading to the neutron $(d_{5/2})^6(d_{3/2}s_{1/2})^4(f_{7/2}p_{3/2})^2$ configurations. This is more evident at the onset of deformation when they are between orbitals across $N = 20$ with spin-differences of two units $\Delta j = 2$. In this case, the spherical closed-shell configuration has a zero particle-zero hole character, whereas the deformed configuration has a two-particle-two-hole configuration from the occupied orbital, $d_{3/2}$, to the empty valence orbital, $f_{7/2}$. The level structure derived from our shell-model calculations is displayed in Fig. 3, in which the constructed level scheme is also in-cluded for comparison. For discussion, we denote the val-ues of the predicted quadrupole transition strengths. Here, the effective charges used were $e_p = 1.5e$ for protons and $e_n = 0.5e$ for neutrons. As is apparent in Fig. 3, the shell model predictions agree well with the experimental data.

In Table 1, we show the calculated probabilities of the main configurations for the states of interest. The ground state is found to exhibit the dominance of both proton (π) and neutron (ν) closed shells, indicating the $\pi(d_{5/2})^6$ $\nu(d_{5/2})^6(s_{1/2})^2(d_{3/2})^4$ configuration with 73%. However, we find that two-neutron excitations from $d_{3/2}$ to $f_{7/2}$, $(d_{3/2})^2(f_{7/2})^2$ contribute as well, which amounts to about 8%. On the contrary, the proton excitations to the $s_{1/2}$ or-bital across $Z = 14$ are negligible. Hence, we see that a large depletion occurs at the center of the proton matter. This toroidal-like structure, sometimes called a bubble structure, in the ground state has been proven experiment-ally by one proton removal reaction [13]. In contrast to the ground state, the excited 2_2^+, 3_1^+, 2_3^+, and 3_2^+ states are produced dominantly by occupations of the proton $s_{1/2}$ orbital. From the ground state to the first 6^+ state through the first 2^+ and 4^+ states, the $\pi(d_{5/2})^6\ \nu(d_{5/2})^6(s_{1/2})^2$ $(d_{3/2})^2(f_{7/2})^2$ component increases rapidly. The calculated 2_1^+, 4_1^+, and 6_1^+ energies are in good agreement with the experimental data. Here, the 6_1^+ state can be understood in terms of full spin alignment of the neutron $f_{7/2}$ orbital. This type of energetically favored state has been com-monly observed as a spin trap caused by a non-collective oblate distribution.

The second 0^+, 0_2^+ state is certainly reproduced in en-ergy by the neutron two particles-two holes $(d_{3/2})^2(f_{7/2})^2$
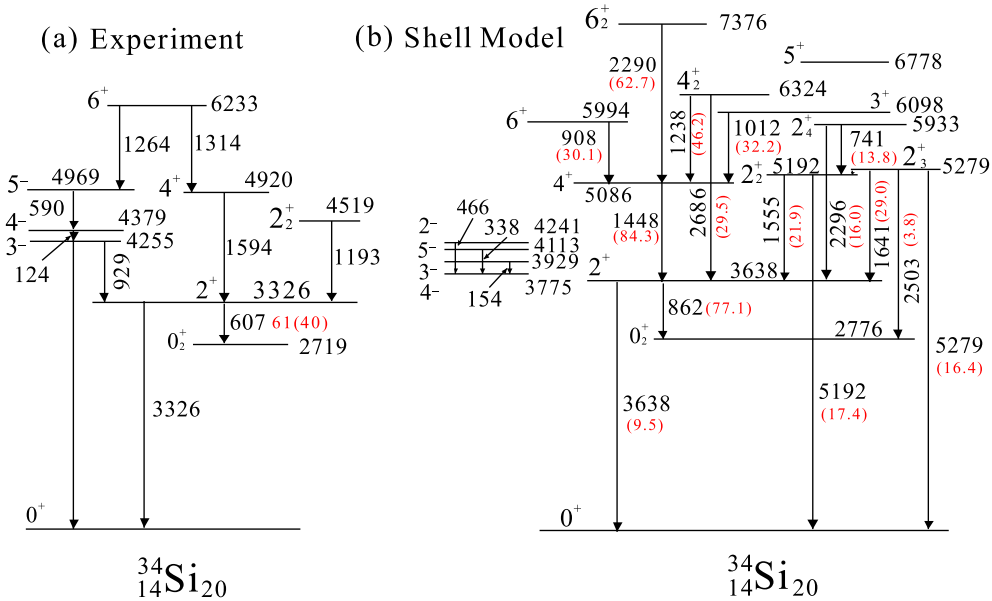

Fig. 3. (color online) (a) Level scheme of ^{34}Si proposed by the present work. (b) The predicted level scheme of ^{34}Si according to the large-scale shell-model calculations over the space of $d_{5/2}$, $s_{1/2}$, $d_{3/2}$, $f_{7/2}$, and $p_{3/2}$ for both protons and neutrons. Numbers in parentheses are the expected electric quadrupole transition strengths, $B(E2; J+2 \rightarrow J)$, in e^2fm^4. The experimental value in (a) is from [6].

configuration, which amounts to about 40%, including a proton $s_{1/2}$ excitation with 9%. Moreover, the expected value, 77 e^2fm^4, of the reduced quadrupole transitional strength, $B(E2;2_1^+$ to $0_2^+)$ is consistent with that of the experimental result, 61(40). According to the monopole strength in [6], this second 0^+ state was found to have a deformation with $\beta = 0.29(4)$. To confirm this result, we investigated a level crossing between the $d_{3/2}$ and $f_{7/2}$ orbitals using a deformed shell model with a stretched harmonic oscillator potential. It is found that the crossing between the $d_{3/2}[2, 2, 3/2, 3/2]$ orbital and the $f_{7/2}[3, 3, 7/2, 1/2]$ orbital occurs around $\varepsilon_2 = 0.22$. Here, [2, 2, 3/2, 3/2] indicates the harmonic oscillator number (N), angular momentum (l), total spin (j), and total spin projection (j_z), respectively, and the quadrupole deformation parameter ε_2 corresponds to $0.95\beta_2$. This result proves the deformation derived from the monopole transition strength.

The negative-parity states 3^-, 4^-, and 5^- located above the 2^+ state are dominated by the neutron one particle-one hole excitation, viz., $(d_{3/2})^{-1}(f_{7/2})^1$ by promoting a neutron from the $d_{3/2}$ orbital to the $f_{7/2}$ orbital, which is the $\pi(d_{5/2})^6\nu(d_{5/2})^6 (s_{1/2})^2 (d_{3/2})^3(f_{7/2})^1$ configuration in the last column of Table 1. This one hole-one particle configuration energetically favors the generation of angular momenta 3^- to 5^- as shown in Fig. 3(b). Even though the ordering of the 3^- and 4^- states is predicted to be reversed, this explains the small energy separation between them. In this configuration, two neutrons, on one hand, as a particle in the $f_{7/2}$ orbital and, on the other hand, as a hole

in the $d_{3/2}$ orbital, yield the maximal spins $J = 5$ (7/2 + 3/2). Then, two neutrons favor organization in a doughnut distribution, as shown in Fig. 4. In contrast to neutrons, no (or little) occupancy of the proton $s_{1/2}$ orbital in these negative-parity states implies that the spherical core has a proton center depletion similar to the ground state. Recently, new experimental results for ^{34}Si were reported [18], and the suggested level structure and shell model descriptions strengthen our discussion of the present work.

A surprising outcome occurs at 6_2^+. Comparing the configurational probabilities between 6_1^+ and 6_2^+, the dominance of the $\pi(d_{5/2})^6\nu(d_{5/2})^6(s_{1/2})^2(d_{3/2})^2(f_{7/2})^2$ configuration, 42%, at 6_1^+ weakens at 6_2^+, 22%. Instead, at the 6_2^+ state, the $\pi(d_{5/2})^5(s_{1/2})^1\nu(d_{5/2})^6(s_{1/2})^2(d_{3/2})^2(f_{7/2})^2$ and $\pi(d_{5/2})^6\nu(d_{5/2})^5(s_{1/2})^1(d_{3/2})^2(f_{7/2})^2$ configurations contribute largely, 14% and 12% (not shown in Table 1), respectively. Such broad contributions, namely the richness of configuration mixing, might induce a deformed collective structure at 6_2^+. In fact, the quadrupole transition of 6_2^+ to 4_1^+ is stronger by two times than that of 6_1^+ to 4_1^+. We find that such strong quadrupole strengths are maintained along the $6_2^+ \rightarrow 4_1^+ \rightarrow 2_1^+ \rightarrow 0_2^+$ cascade with values near $60 - 80$ e^2fm^4, which are 10 to 13 times the Weisskopf single-particle transition unit. Further, the cascading energies, 2290-1448-862 keV, definitely show a rotational pattern. We propose a deformed rotational band built on the second 0^+, as shown in Fig. 3(b). To confirm our suggestion, the second 6^+ state needs to be identified

Table 1. Shell model calculations for contributions, %, of the orbital configurations of ^{34}Si. The shell model is based on the sdfp-m interaction including $2\hbar\omega$ pf shell two particle-two hole excitations.

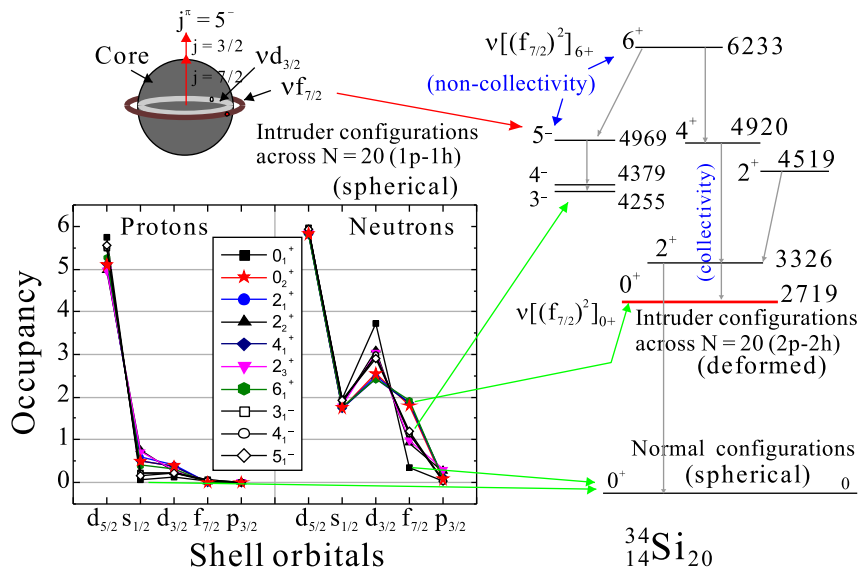|	$\pi(d_{5/2})^6$ $\nu(d_{5/2})^6 (s_{1/2})^2$ $(d_{3/2})^4$	$\pi(d_{5/2})^6$ $\nu(d_{5/2})^6 (s_{1/2})^2$ $(d_{3/2})^2(f_{7/2})^2$	$\pi(d_{5/2})^5(s_{1/2})^1$ $\nu(d_{5/2})^6 (s_{1/2})^2$ $(d_{3/2})^4$	$\pi(d_{5/2})^5(s_{1/2})^1$ $\nu(d_{5/2})^6 (s_{1/2})^2$ $(d_{3/2})^2(f_{7/2})^2$	$\pi(d_{5/2})^6$ $\nu(d_{5/2})^6 (s_{1/2})^2$ $(d_{3/2})^2(f_{7/2})^1(p_{3/2})^1$	$\pi(d_{5/2})^5(s_{1/2})^1$ $\nu(d_{5/2})^6 (s_{1/2})^2$ $(d_{3/2})^3(f_{7/2})^1$	$\pi(d_{5/2})^6$ $\nu(d_{5/2})^6 (s_{1/2})^2$ $(d_{3/2})^3(f_{7/2})^1$
0^+	73	8					
2^+		26		13			
4^+		31		9			
6^+		42		6			
0_2^+	6	29		9			
2_2^+		10	34	7			
3_1^+			24	9	7		
4_2^+		17		10	9		
2_3^+		8	30		10		
3_2^+			36	9	5		
2_4^+		32		6	8		
5^+					22		
6_2^+		22		14			
1^+		26		10			
3^-						5	61
4^-						5	62
5^-							65

Fig. 4. (color online) Occupancies of the orbitals involved in the states observed in ^{34}Si. Following the shell model results, some distinctive structures are indicated in the level scheme.

by an experiment. Interestingly, we find a γ-ray peak at and near 1940 keV in Fig. 2 in Ref. [5], where the coincidence γ-ray spectra gated on the 3326 and 929-keV transitions are displayed. We suggest that this peak might be the γ-ray transition of the 6_2^+ state, which corresponds to the 6860-keV level, to the 4^+ state at 4920 keV. It is also interesting to find a close resemblance between the collective bands, the 6_2^+ - 4_1^+ - 2_1^+ - 0_2^+ sequence in ^{34}Si and the 6_2^+ - 4_1^+ - 2_2^+ - 0_2^+ sequence in ^{38}Ar.

A spherical ground band consists of the 2_2^+ and 4_3^+ states. The doubly magic nature of ^{34}Si is indicated by the high energy positions of the 2_2^+ state at 4.519 MeV and the 3^-, 4^-, and 5^- states of the one-particle one-hole cross-shell states at around 4.5 MeV, and the calculated $E(4_3^+/2_2^+) = 1.38$. As a doubly magic nucleus, the 2^+ state of the spherical ground band has the highest energy among all even-even nuclei with $Z = 10 \sim 18$ [1]. In this view, all excitation states stay relatively high with a small $E(4^+/2^+)$ value compared with other nuclei. The structure of ^{34}Si is similar to that of many spherical nuclides with a large shell gap (magic shells), such as ^{68}Ni [1].

In another view, taking the 0_2^+ state as a reference, $E(4_1^+/2_1^+) = 2.68$ is calculated, indicating certain deformation and a possible γ-soft nature, as shown with the $O(6)$ limit of the interacting boson model (IBM) [19, 20]. Such observations show the co-existence structure of ^{34}Si, with the spherical 0_1^+ state and deformed 0_2^+ state. Combining the observed data, the present shell-model calculation, IBM, and the discussion in Ref. [18], the 0_2^+, 2_1^+, 4_1^+, and 6_2^+ states belong to a deformed band of γ-soft nature, while the 2_3^+, 3_1^+, and 4_2^+ states can be assigned to the corresponding γ-vibrational band.

As seen in Table 1, all 0_2^+, 2_1^+, 4_1^+, and 6_2^+ states have a similar configuration and structure, forming a rota-

tional band with strong in-band transitions. A γ-soft state should have certain large transition strengths from states outside the band because of the mixing between different bands. As seen from the shell-model results, all 2^+ states except for the 2_1^+ state have extremely weak transition strengths to the 0_2^+ state. For the 2_1^+ and 4_1^+ states, several states decay to them with transition strengths of 30 ∼ 40 e^2fm^4. Table 2 compares the $B(E2)$ transitions between the present shell-model calculation and the IBM $O(6)$ limit. The transition rates generally agree with the $O(6)$ limit for $4_1^+ \rightarrow 2_1^+$, $3_1^+ \rightarrow 4_1^+$, $4_2^+ \rightarrow 2_1^+$, and $4_2^+ \rightarrow 4_1^+$. However, for the transition rates related to the 2_3^+ state, the deviations between the shell model and the $O(6)$ limit become large. The energies and $B(E2)$ values for the γ-soft states are rather consistent with the $O(6)$ limit, though there seems to be a certain mixing between the $K = 0$ and $K = 2$ bands. More γ-ray transitional investigations, namely timing measurements, are essential for understanding ^{34}Si, especially the possible γ-soft rotational band and the mixing between different bands.

IV. CONCLUSION

In conclusion, we successfully develop the existing level scheme of ^{34}Si by assigning spin-parities up to 6^+ to the available experimental data. Figure 4 summarizes our results by showing distributions of the orbital occupancies for the states of interest together with the constructed level scheme. The observed states could be understood by finding certain differences in both the occupancies and contributions of the respective shell configurations as well as the resultant transition strengths. For example, the dominance of either protons or neutrons and the extent of mixing of their configurations are directly

Table 2. Shell model calculations for $E2$ transitions and comparison with IBM $O(6)$ limit.

$J_i \rightarrow J_f$	Shell-model $B(E2)$ in unit e^2fm^4	Shell-model $B(E2)$ in unit $B(E2; 2_1^+ \rightarrow 0_2^+)$	IBM $O(6)$ limit $B(E2)$ in unit $B(E2; 2_1^+ \rightarrow 0_2^+)$
$2_1^+ \rightarrow 0_2^+$	77.1	1	1
$4_1^+ \rightarrow 2_1^+$	84.3	1.09	$10/7 \approx 1.43$
$6_2^+ \rightarrow 4_1^+$	62.7	0.81	$5/3 \approx 1.67$
$4_2^+ \rightarrow 2_3^+$	16.7	0.22	$55/63 \approx 0.87$
$3_1^+ \rightarrow 2_3^+$	34.9	0.45	$25/21 \approx 1.19$
$3_1^+ \rightarrow 4_1^+$	32.2	0.42	$10/21 \approx 0.48$
$2_3^+ \rightarrow 2_1^+$	29.0	0.38	$10/7 \approx 1.43$
$4_2^+ \rightarrow 2_1^+$	29.5	0.38	0
$4_2^+ \rightarrow 4_1^+$	46.2	0.60	$50/63 \approx 0.79$

related to an understanding of the emerging features, i.e., nuclear shapes, singles or collective degrees of freedom, and specific matter distributions. As denoted by the collectivity and non-collectivity in Fig. 4, the distinctive level properties are noted; a proton center depletion due to the empty $s_{1/2}$ orbital of the spherical ground state, a neutron two particle-two hole, $(d_{3/2})^{-2}(f_{7/2})^2$ configuration in the deformed second 0^+ state, a neutron one hole-one particle, $(d_{3/2})^{-1}(f_{7/2})^1$ configuration for the negative parity states, and non-collective fully-aligned spin states, $\nu[(d_{3/2})^{-1}(f_{7/2})^1]_{5-}$ and $\nu[(f_{7/2})^2]_{6+}$. The proposed rotational band, as predicted by the second 6^+ state, is built on the second 0^+ state in ^{34}Si and provides new insights into shape co-existence in isotones with $N = 20$; ^{32}Mg, ^{36}S, ^{38}Ar, and ^{40}Ca.

References

[1] National Nuclear Data Center, Brookhaven National Laboratory, "NuDAT 2.7", https://www.nndc.bnl.gov

[2] P. Baumann, A. Huck, G. Klotz *et al*., Phys. Lett. B **228**, 458 (1989)

[3] R. W. Ibbotson, T. Glasmacher, B. A. Brown *et al*., Phys. Rev. Lett. **80**, 279 (1998)

[4] S. Nummela, P. Baumann, E. Caurier *et al*., Phys. Rev. C **63**, 044316 (2001)

[5] S. Paschalis, P. Fallon, A. O. Macchiavelli *et al*., Journal of Physics:Conference Series **312**, 092050 (2011)

[6] F. Rotaru, F. Negoita, S. Grévy *et al*., Phys. Rev. Lett. **109**, 092503 (2012)

[7] N. Iwasa, T. Motobayashi, H. Sakurai *et al*., Phys. Rev. C **67**, 064315 (2003)

[8] R. Lică, F. Rotaru, M. J. G. Borge *et al*., Physics. Rev. C **95**, 021301(R) (2017)

[9] R. Han, X. Q. Li, W. G. Jiang *et al*., Phys. Lett. B **772**, 529 (2017)

[10] E. Caurier, F. Nowacki, A. Poves *et al*., Phys. Rev. C **58**, 2033 (1998)

[11] Yutaka Utsuno, Takaharu Otsuka, Takahiro Mizusaki *et al*., Phys. Rev. C **46**, 011301(R) (2001)

[12] M. Grasso, L. Gaudefroy, E. Khan *et al*., Phys. Rev. C **79**, 034318 (2009)

[13] A. Mutschler, A. Lemasson, O. Sorlin *et al*., Nature Physics **13**, 142 (2017)

[14] T. Duguet, V. Somà, S. Lecluse *et al*., Phys. Rev. C **95**, 034319 (2017)

[15] Y. Utsuno, T. Otsuka, T. Mizusaki *et al*., Phys. Rev. C **60**, 054315 (1999)

[16] Noritaka Shimizu, *Nuclear shell-model code for massive parallel computation, KSHELL*, arXiv: 1310.5431 (2013)

[17] S. Noritaka, M. Takahiro, U. Yutaka *et al*., Comput. Phys. Commun. **244**, 372-384 (2019)

[18] R. Lică, F. Rotaru, M. J. G. Borge *et al*., Phys. Rev. C **100**, 034306 (2019)

[19] F. Iachello and A. Arima, The interacting boson model, Cambridge, (1987)

[20] R. F. Casten, Nat. Phys. **2**, 811 (2006)